Available online at www.sciencedirect.com
ScienceDirect
European Polymer Journal 44 (2008) 1275–1284
EUROPEAN POLYMER JOURNAL
www.elsevier.com/locate/europolj

Macromolecular Nanotechnology

Effect of the intercalated cation on the properties of poly(*o*-methylaniline)/maghnite clay nanocomposites

Horacio J. Salavagione [a], Diego Cazorla-Amorós [b], Selma Tidjane [c], Mohammed Belbachir [c], Abdelghani Benyoucef [d], Emilia Morallón [a,*]

[a] *Universidad de Alicante, Departamento de Química Física e Instituto Universitario de Materiales, Apartado 99, 03690, Alicante, Spain*
[b] *Universidad de Alicante, Departamento de Química Inorgánica, Apartado 99, E-03080 Alicante, Spain*
[c] *Université d'Oran Es-Senia, Département de Chimie, Faculté des Sciences, BP 1524, El M'nouar, 31000 Oran, Algeria*
[d] *Centre Universitaire de Mascara, Inst. des Sciences et Technologies, BP 630 29000-Mascara, Algeria*

Received 21 December 2007; accepted 31 January 2008
Available online 15 February 2008

Abstract

A detailed study about the synthesis, characterization and properties of poly(*o*-methylaniline)(PoMea)/maghnite nanocomposites has been performed. Changes in the characteristics of the nanocomposites, depending on the intercalated cation between the clay layers before the synthesis, have been observed. Intercalated morphology has been detected by TEM in nanocomposites containing copper-treated maghnite (Magh-Cu), while when maghnite treated with strong acids was used (Magh-H); an exfoliated material has been obtained. Also, remarkable differences in the properties of the polymers have been observed by TG-MS and FTIR, suggesting that the polymer produced with Magh-H has a higher degree of branching. The electrochemical behavior of the polymers extracted from the nanocomposites has been studied by cyclic voltammetry. Good electrochemical response has been observed for PoMea grown into Magh-Cu but not for the one polymerized into Magh-H.

Keywords: Maghnite clay; Nanocomposite; Conducting polymers; Montmorillonite clay; Poly(*o*-methylaniline)

1. Introduction

Among the conducting polymers, polyaniline is the most studied because of its remarkable thermal and environmental stability and low cost production [1]. Nowadays, polyaniline (PANI) and its derivatives find potential applications as flat panels, electro magnetic interference (EMI) shielding [2], lightweight batteries, organic field effect transistors (FETs) [3], sensors [4], printed boards, etc. The production of polymers and composites with nanostructured shape is a subject of great interest. In this sense, nanoparticles of PANI and its derivatives were produced by polymerization in emulsion [5–8]. Huang and Kanner reported the synthesis of PANI nanofibers by phase transfer polymerization [9,10]. Furthermore, PANI was synthesized into the channels of inorganic hosts [11–13], generally, by absorbing the monomer in the host and then adding the oxidant. Among these, the host most commonly

* Corresponding author. Tel.: +34 965909590; fax: +34 965903537.
E-mail address: morallon@ua.es (E. Morallón).

0014-3057/$ - see front matter © 2008 Elsevier Ltd. All rights reserved.
doi:10.1016/j.eurpolymj.2008.01.042

used for polymer nanocomposites are expandable-layered silicates, being maghnite (Magh, a natural sodium montmorillonite clay obtained from Tlemcen (Algeria)) a typical example. Polymer/layered silicate nanocomposites can either be intercalated, if the polymer is present between the silicate layers and the regularity of the layered structure is maintained, or exfoliated if the silicate layers are completely dispersed into the matrix.

Polymer/montmorillonite nanocomposites have attracted considerable attention because they are expected to increase the degree of polymer ordering. Montmorillonite clay is a layered inorganic material, composed of silicate layers 1 nm thick and 200–300 nm in the lateral dimension. Thus, the mechanical, optical, electronic and chemical properties of the polymer, as well as the thermal stability can be enhanced because of the formed nanostructure scale, the strong interaction between the polymer and the silicate layers, and the large surface area of the montmorillonite clay.

Composites of several conducting polymers with montmorillonite were synthesized under different conditions [12–23]. Temperini et al. monitored the polymerization of aniline, intercalated into sodium-montmorillonite; they found differences between the structure of the polymer in the nanocomposite and bulk PANI [14,18]. Using resonance Raman and XANES they suggested the formation of benzidine segments and azo bonds in addition to the typical PANI structure formed by head-to-tail coupling [14,18].

Furthermore, montmorillonite constitutes of two dimensional silicate anions with cations between the layers that can be easily exchanged. Thus, the interlayer spacing can be modified, depending on the cation intercalated. Taking profit of the swelling of the montmorillonite when it is immersed in water that produces a remarkable increase of the interlayer spacing [24], Yoshimoto et al. explored the mechanochemical intercalation of different anilinium salts (chloride, fluoride and sulphate) into sodium montmorillonite layers prior to the polymerization [12,13,19]. They concluded that nanocomposites made using a solvent-free mechanochemical method produced much more polyaniline between the montmorillonite layers than that obtained by conventional solution methods. On the other hand, PANI doped with voluminous counterion (dodecylbenzenefulfonic acid, DBSA) was synthesized into sodium montmorillonite by intercalating the anilinium-DBSA salts in the MMT layers prior the polymerization [15]. The authors suggested that the montmorillonite weakens the polymer interchain interaction and increases the disorder, which results in lower values of conductivity.

However, in the studies described above, only sodium treated montmorillonite was employed. Therefore, the use of modified montmorillonite with different inorganic cations can affect the properties of the nanocomposites and polymers and merits research efforts.

For this purpose, in this work we report the synthesis of nanocomposites of poly(*o*-methylaniline) (PoMea) with a natural montmorillonite (maghnite) clay modified with two inorganic cations (i.e., H^+ and Cu^{2+}) and the properties of the nanocomposites and the polymers extracted from them.

2. Experimental

The *o*-methylaniline was purchased from Aldrich and used as received. Perchloric acid (from Merck) was suprapure quality and the water employed for the preparation of the solutions was obtained from Elga Labwater Purelab Ultra system.

A natural sodium montmorillonite clay (named as maghnite) obtained from Tlemcen (Algeria) has been used. In a typical experiment, the sodium maghnite (Magh-Na) was treated with 0.25 M H_2SO_4 solution (called Magh-H). After filtration the Magh-H was dried at 105 °C overnight and its composition was measured by X-ray fluorescence, obtaining the data in Table 1. To obtain maghnite with copper intercalated (Magh-Cu), the Magh-H was dispersed into a 1 M $CuCl_2$ solution and stirred for 24 h. Then the solid was recovered by centrifugation and washed with abundant water. The absence of chloride was confirmed using silver nitrate. The products were dried at 110 °C.

To obtain the nanocomposites, 0.022 mol of *o*-methylaniline were added to 1 g of the clay and

Table 1
Composition of Magh-Na treated with 0.25 M H_2SO_4 (wt%) (Magh-H)

SiO_2	Al_2O_3	Fe_2O_3	CaO	MgO	Na_2O	K_2O	TiO_2	SO_3
71.70	14.03	0.71	0.28	0.80	0.21	0.77	0.15	0.34

the mixture was kept under magnetic stirring for 1 h. The chemical polymerization began when 100 ml of 0.1 M sodium peroxodisulfate solution was slowly added to the mixture. Thus, the final concentration of *o*-methylaniline was 0.22 M. The reaction was carried out under magnetic stirring for 1 h at room temperature. The nanocomposites were isolated, washed with acetone, 1 M hydrochloric acid and then dried at 60 °C for 24 h.

For TEM experiments, the nanocomposites were dispersed in water and then cast in TEM grids. The images were collected using a JEOL (JEM-2010) microscope, working at an operation voltage of 200 kV.

The X-ray diffraction of the powder nanocomposites were taken using a Bruker CCD-Apex equipment with a X-ray generator (Cu Kα and Ni filter) operated at 40 kV and 40 mA. X-ray fluorescence spectroscopy of the powder nanocomposites was made using a Philips PW1480 equipment with a UNIQUANT II software to determine elements in a semi quantitative way. The chemical analysis was made with a Rontec X-ray detector for energy dispersive X-ray microanalysis (EDX). The thermogravimetric analysis (TGA) was carried out using a Mettler Toledo 851E/1600/LG equipment. The samples were dried under dynamic vacuum before the experiments and then placed in an alumina crucible of 70 μl. The weight change was monitored from room temperature to 1000 °C using a heating rate of 10 °C/min. The experiments were carried out in He.

Fourier transform infrared (FTIR) spectra of the composites, in the transmission mode, were obtained in KBr pellets using a Nicolet Magna equipment with a 4 cm^{-1} resolution.

For conductivity measurements, the powder nanocomposites were doped by putting in 1 M HCl solution during 12 h, then filtered and dried under vacuum.

The electrochemical behavior of the polymers was studied by cyclic voltammetry after their extraction from the nanocomposites by dissolving in the *N*-methyl-2-pyrrolidone (NMP). It is known that this kind of conducting polymer is soluble in NMP [25], while the clay remains in solid state. Thus, both components can be separated by filtration. The electrochemical measurements were carried out using a conventional cell of three electrodes. The counter and reference electrodes were a platinum foil and a hydrogen reversible electrode immersed in the same electrolyte, respectively. The working electrode was prepared as follows: after the polymer was extracted from the nanocomposite using NMP, 50 μl of this solution were cast over platinum disks and the solvent evaporated to create polymeric films. The electrolyte used was 1 M $HClO_4$ and all experiments were carried out at 50 mV s^{-1}.

3. Results and discussion

Maghnite clay with two intercalated inorganic cations was prepared as described in Section 2. The copper modified maghnite (Magh-Cu) and the protonated maghnite (Magh-H) were characterized using X-ray diffraction to check changes in the interlayer spacing (Fig. 1a). The XRD patterns show that the (0 0 1) diffraction peak between 6° and 7° changes depending on the inorganic cation intercalated. Table 2 includes the *d*-spacing between the montmorillonite sheets calculated from the Bragg equation, the ionic radii, the solvated radii and the maximum 2θ of the peaks; this table shows that the size of the solvated cation rather than the ionic size determines the layer expansion [27].

The diffraction patterns of PoMea/Magh-Cu and PoMea/Magh-H nanocomposites are shown in Fig. 1b. Table 3 summarizes the XRD data obtained. Although the diffraction pattern is similar for both samples, the (0 0 1) diffraction peak for PoMea/Magh-Cu has a shoulder at lower angles ($2\theta = 5.6°$). While PoMea/Magh-H nanocomposites have a basal spacing of 14.3 Å (which is higher than that for Magh-H, Table 2), PoMea/Magh-Cu has two basal spacing at 14.3 and 15.8 Å suggesting the intercalation of some PoMea chains between the maghnite layers. Yoshimoto et al. observed a similar change in the diffraction peak when they intercalated different amounts of anilinium salts into montmorillonite layers [13]. They attributed it to the existence of two types of conformation of intercalated species controlled by the anilinium concentration [13]. Thus, in a similar way, the PoMea/Magh-Cu sample can lead to different structures with different basal spacing. The EDX data proves the presence of around 0.5 wt% of copper in PoMea/Magh-Cu (Table 4). Considering that the starting sodium montmorillonite has a cation exchange capacity of 1.15×10^{-3} mol g^{-1} [13] and knowing that the cation incorporated carries two positive charges, the theoretical weight percent of copper before polymerization should be 3.65 wt%. The experimental value obtained from EDX is

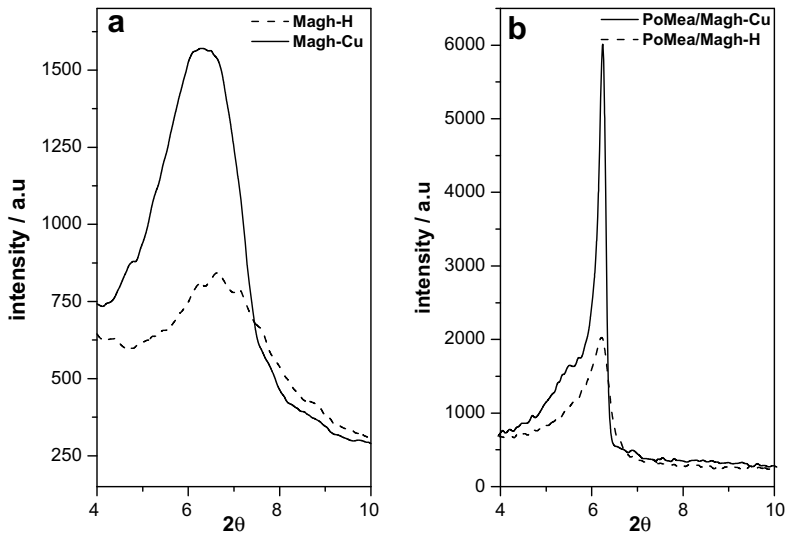

Fig. 1. XRD diffraction patterns of (a) copper (Magh-Cu) and protonated montmorillonite (Magh-H) and (b) PoMea/Magh-Cu and PoMea/Magh-H nanocomposites.

Table 2
Ionic radii, peak maximum and *d*-spacing of different cations intercalated into maghnite

Ion	Ionic radii[b] (Å)	Stokes radii[a] (Å)	Peak maximum, $2\theta_{max}$	Basal spacing, $d_{(001)}$ (Å)	Interlayer spacing[c], Δd (Å)
Na^+	1.02	1.63	7.01	12.3	2.6
Cu^{2+}	0.73	5.79	6.42	13.8	4.1
H^+	–	–	6.7	13.2	3.5

[a] Calculated data.
[b] Data obtained from [26].
[c] Thickness of a montmorillonite layer = 9.7 Å [15].

Table 3
Peak maximum and *d*-spacing of the nanocomposites

Nanocomposite	Peak maximum, $2\theta_{max}$ (deg)	Basal spacing, $d_{(001)}$ (Å)	Interlayer spacing[a], Δd (Å)
PoMea/Magh-H	6.2	14.3	4.6
PoMea/Magh-Cu	6.2	14.3	4.6, 0.5[b]
	5.6	15.8	6.1, 2.0[b]

[a] Thickness of a montmorillonite layer = 9.7 Å [15].
[b] Related to Magh-Cu spacing from Table 2.

2.8 wt% (Table 4), which corresponds to a 77% of ion exchange. Therefore, almost a third part of the Cu cations remain into the clay layers after polymerization.

TEM images of PoMea/Magh-H and PoMea/Magh-Cu nanocomposites are shown in Fig. 2.

Table 4
Experimental data obtained by energy dispersive X-ray microanalysis (EDX)

Sample	S (wt%)	Cu (wt%)	Na (wt%)
Magh-H	–	–	1.1
Magh-Cu	–	2.8	0.4
PoMea/Magh-H	14.4	–	–
PoMea/Magh-Cu	8.7	0.5	–

Remarkable differences exist in the morphology of the composites; while PoMea/Magh-Cu presents an intercalated structure (Fig. 2a), PoMea/Magh-H appears mainly as an exfoliated material (Fig. 2b). The separations between clay layers in PoMea/Magh-Cu were measured using image-processing software. Essentially, three different separations at 10.5, 14 and 16 Å were detected, being the first and the most abundant (about 40%). The first value is close to that reported for sodium montmorillonite [13]. Furthermore, the other distances (14 and 16 Å, 20% each) resemble those obtained for PoMea/Magh-Cu from XRD data (Table 3). Therefore, it is possible that polymerization of *o*-methylaniline occurs only into a part of the clay layers, while the other galleries remain filled with copper, in agreement with the EDX analysis in Table 4. Beyond this, it is evident that the type of cation occupying the maghnite channels before the polymerization influences the morphology of the composites. When Magh-H is used the clay layers are

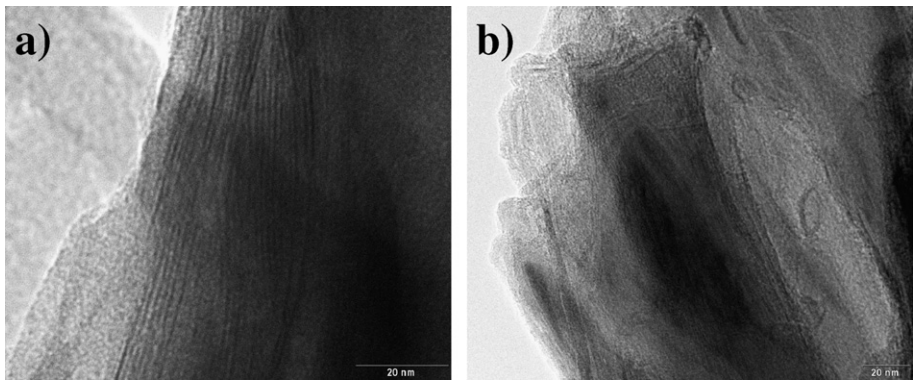

Fig. 2. TEM images of (a) PoMea/Magh-Cu and (b) PoMea/Magh-H.

not parallel to each other, giving a non-oriented structure and the lack of the shoulder at lower angles in XRD for PoMea/Magh-H could be due to the exfoliation that decreases the angle to values outside the limit of the equipment. The exfoliation can be explained as follows: (1) the cation exchange capacity of Magh-H could be higher than Magh-Cu. Thus, more anilinium salt is present into the clay galleries before the polymerization and consequently more polymer is produced. (2) PoMea produced into Magh-H could be higher in molecular weight or more branched than that made into Magh-Cu.

To analyze the thermal stability of the polymers and nanocomposites, thermogravimetric analysis coupled to mass spectrometry (TG-MS) was performed. Fig. 3 contains the experiments done for Magh-H and Magh-Cu samples. The experiments contain the typical features for montmorillonite, that is, two main endothermal processes at around 75 and 605 °C. The first one corresponds to the evolution of weakly bonded water molecules while the second one to dehydroxylation of the octahedral sheet as demonstrated from the evolved gasses [28].

Figs. 4 and 5 include the TG-MS experiments for the nanocomposites PoMea/Magh-H and PoMea/Magh-Cu, respectively. The thermal behavior of both nanocomposites is similar showing two main processes at around 150 °C and 270 °C and a continuous weight loss at higher temperatures (Figs. 4a and 5a). The first process can be due to evolution of adsorbed molecules such as water and monomers of *o*-methylaniline that have not polymerized, in agreement with the observations of $m/z = 17$, $m/z = 18$ and $m/z = 106$ in both cases (Figs. 4b and 5b). The second process at about 270 °C can be attributed to chemical reactions involving bond scission such as exclusion of amine groups or methyl groups as it happens in poly(aniline-co-*o*-methylaniline) [29] and methoxyl groups in poly(*o*-methoxyaniline) [30], as suggested by the mass spectrometer signals for $m/z = 14$ and $m/z = 15$ (Figs. 4c and 5c). However, additional peaks for $m/z = 18$, $m/z = 32$ and $m/z = 64$ are also observed at around 270 °C (Figs. 4c, d and 5c, d). The peaks at $m/z = 18$ and $m/z = 64$ can be attributed to degradation of the polymer or further monomer oxidation, while the peak at $m/z = 32$ can be attributed to O_2 coming from $Na_2S_2O_8$ since it starts to decompose at around 180 °C [31]. EDX microanalysis confirms the presence of around 4.4 wt% and 8.7 wt% of sulphur in PoMea/Magh-H and PoMea/Magh-Cu, respectively. Also, in both nanocomposites a peak of $m/z = 15$ is observed at higher temperatures (ca. 580 °C) and can be due to ammonia elimination from polymer pyrolysis.

However, the thermal behavior is quite different for PoMea extracted from the nanocomposites, although the main processes described above can also be observed for the extracted polymers. Interestingly, the main weight loss observed for the extracted polymers occurs at higher temperatures than for the nanocomposites (compare Figs. 6 a, b and Figs. 4a and 5a), which reflects a catalytic effect of the maghnite in the polymer decomposition. Additionally, clear differences between both extracted polymers can be observed from the weight loss curves (Figs. 6a and b). Thus, the weight loss of the PoMea from Magh-Cu happens in two well-defined processes at about 200 and 400 °C (Fig. 6a), whereas in the case of PoMea from Magh-H, the weight loss occurs through a more continuous curve and the process at 200 °C cannot be distinguished. These differences in the

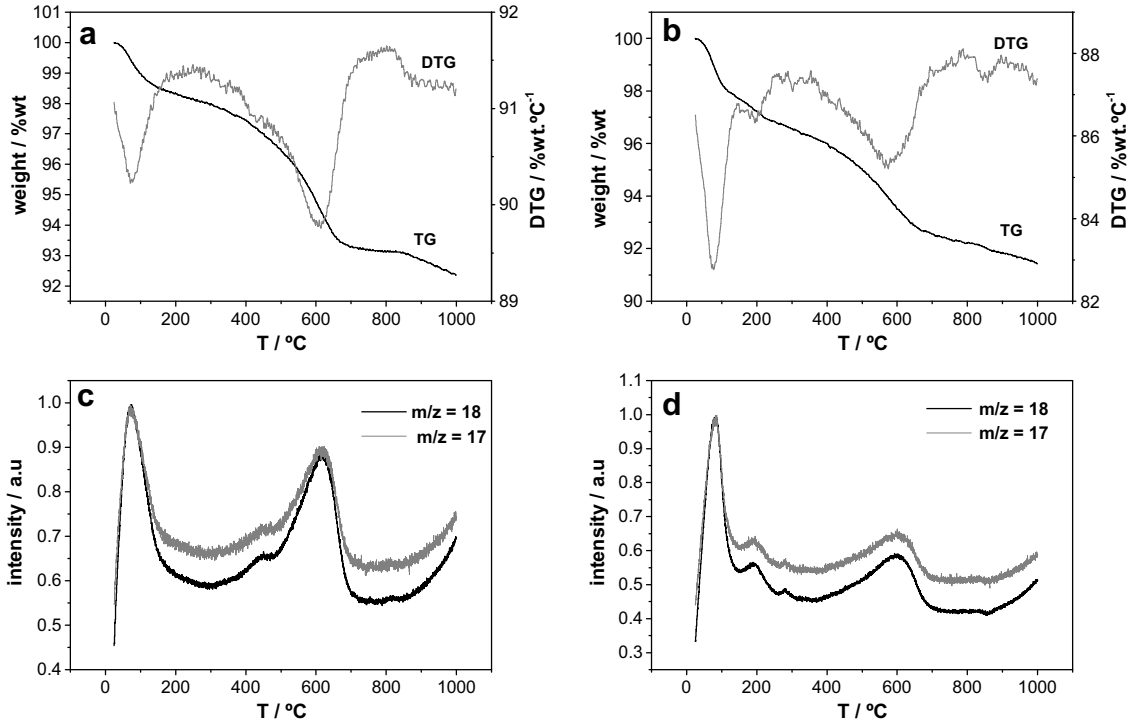

Fig. 3. Thermogravimetry (TG) and differential thermogravimetry (DTG) curves in He for Magh-H (a) and Magh-Cu (b) and evolved gases of Magh-H (c) and Magh-Cu (d).

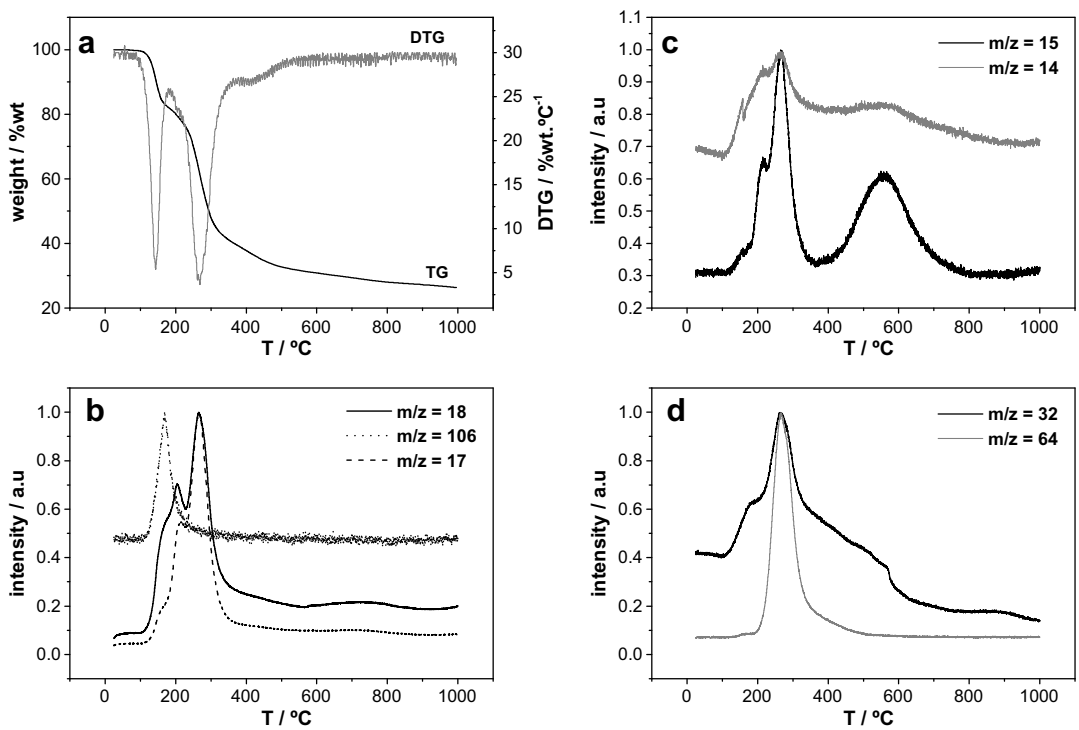

Fig. 4. Thermogravimetry (TG) and differential thermogravimetry (DTG) curves (a) and evolved gases (b–d) for PoMea/Magh-H in He.

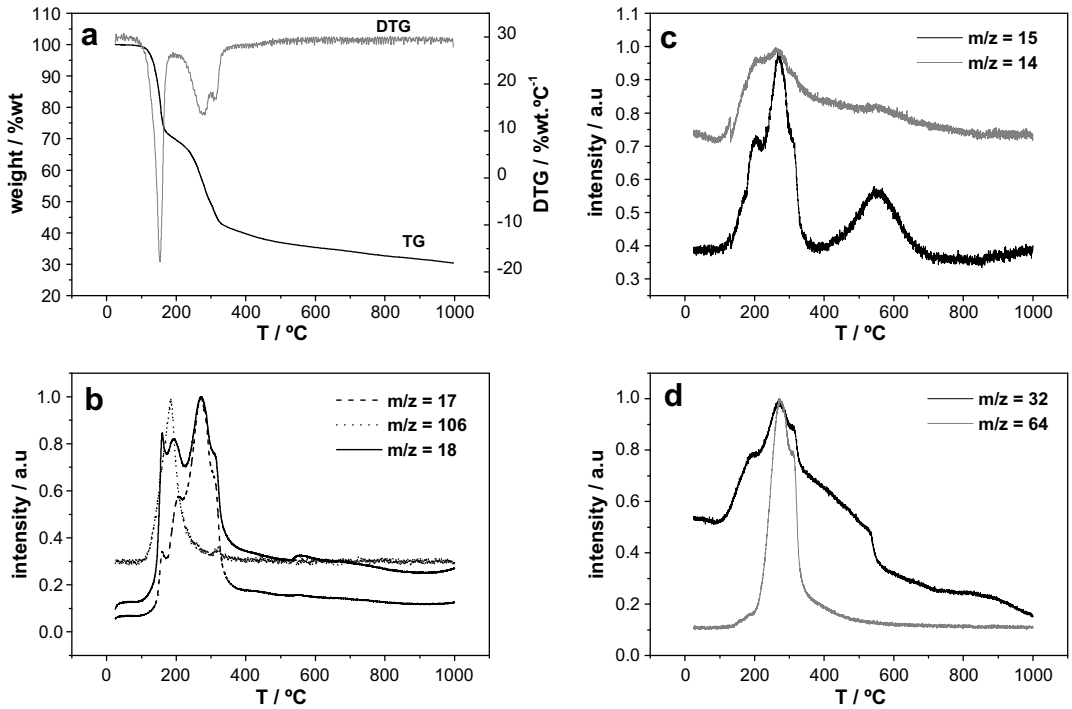

Fig. 5. Thermogravimetry (TG) and differential thermogravimetry (DTG) curves (a) and evolved gases (b–d) for PoMea/Magh-Cu in He.

decomposition of the polymers suggest that they have important differences in the chain structure, having the polymer from Magh-H a higher degree of branching than that from Magh-Cu.

FTIR spectroscopy was used to check the structure of the polymer in the nanocomposite (Fig. 7). As can be seen, the spectra for both nanocomposites (PoMea/Magh-Cu and PoMea/Magh-H) are almost identical and show most of the bands of similar conducting polymers [32]. The band wavelengths and assignments are listed in Table 5. The bands corresponding to montmorillonite vibrations appear at around 1040 and 925 cm^{-1}, which is in agreement with polyaniline/montimorillonite nanocomposites [13]. Also, the structure of PoMea seems to be independent of the cation modifying montmorillonite before the polymerization. However, the broad band starting at around 1900 cm^{-1} that corresponds to electronic transition in the free carriers of the polymer (directly related to the conductivity) [32,33] is higher in PoMea/Magh-Cu than in PoMea/Magh-H, suggesting that PoMea/Magh-Cu has higher electrical conductivity than PoMea/Magh-H. However, pellets of both nanocomposites did not give any significant conductivity. Also, cyclic voltammetry of both composites on platinum electrodes showed no response, suggesting the presence of electroinactive materials.

Therefore, PoMea was extracted from both nanocomposites by dissolving it in NMP (see Section 2). The cyclic voltammograms of PoMea extracted from PoMea/Magh-Cu and PoMea/Magh-H composites in 1 M $HClO_4$ solution are shown in Fig. 8. The current densities have been normalized for a better comparison of both polymers, because the thickness of the films could vary from different samples. Fig. 8 shows that there are remarkable differences. Thus, the PoMea produced from Magh-Cu is electroactive; however, no redox processes are observed for the same polymer from PoMea/Magh-H. For PoMea/Magh-Cu, a broad anodic peak at 0.72 V appears and two reduction peaks (at 0.44 V and around 0.6 V) are observed in the reverse scan, which suggest the existence of two redox processes as occurs in most ring-substituted polyaniline [34–36].

It should be noted that a similar behavior for poly(*o*-methoxyaniline) synthesized into maghnite clay was observed by in-situ Raman spectroscopy, suggesting the existence of a semiquinoid intermediate, which is formed in the first redox process and the oxidation is finished in the second one [21].

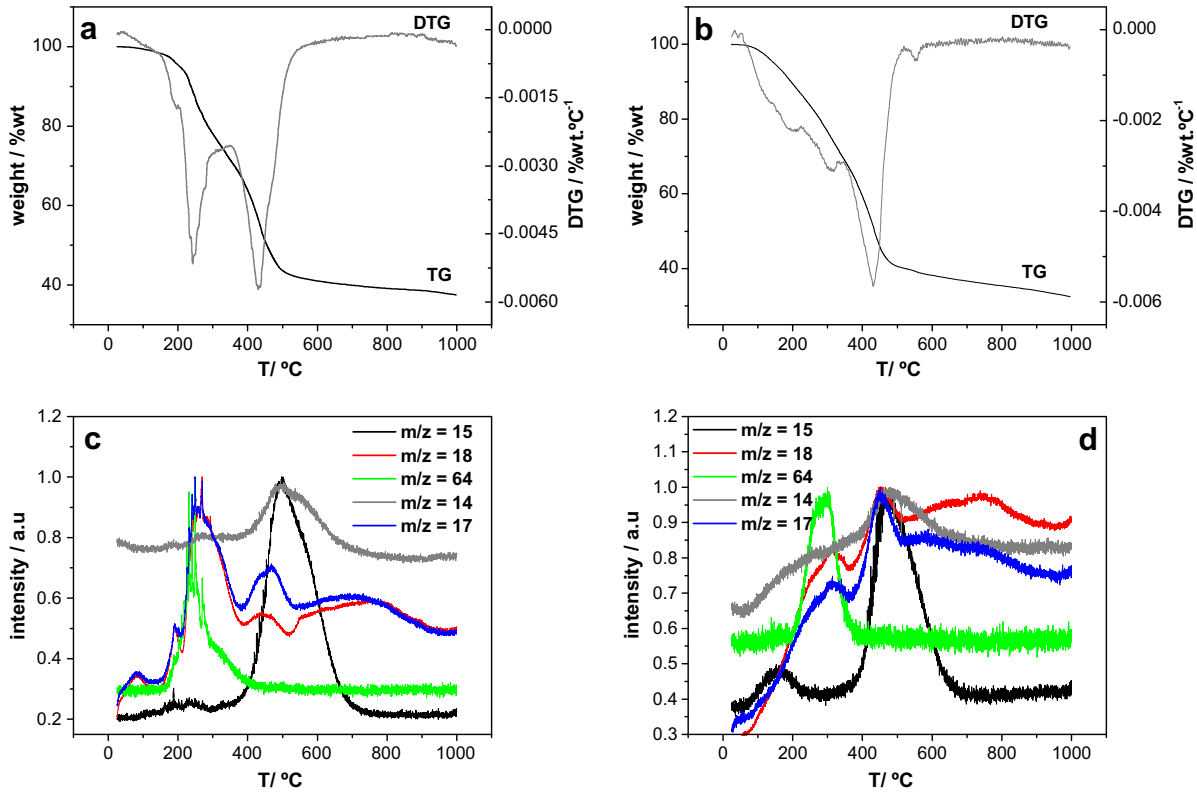

Fig. 6. Thermogravimetry (TG) and differential thermogravimetry (DTG) curves in He for PoMea created into Magh-H (a) and Magh-Cu (b) and evolved gases of the polymer created into Magh-H (c) and Magh-Cu (d).

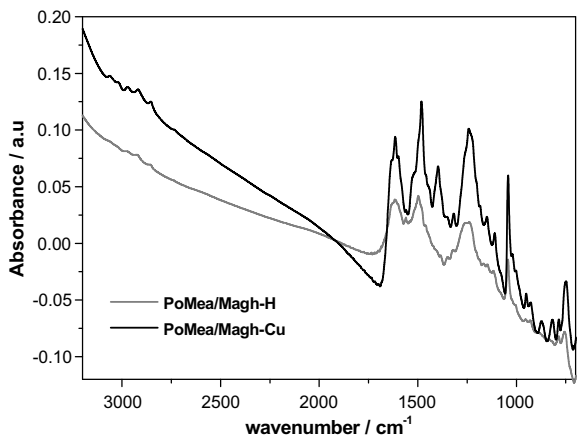

Fig. 7. FTIR transmission spectra of PoMea/Magh-Cu (grey line) and PoMea/Magh-H (black line).

Furthermore, the same behavior was proposed using quartz crystal microbalance and probe beam deflection coupled to the electrochemical systems, for polyaniline [37] and poly(*o*-methylaniline) [38]. Therefore, we can conclude that in poly(*o*-methylaniline) created into Magh-Cu a similar behavior takes place, and that the broad anodic peak consists on the overlapping of two redox processes. The overlapping of peaks also occurs in polyaniline modified with self-doping groups as the pH of the electrolyte increases [39], suggesting that protons are involved in the redox mechanism.

On the contrary, films of PoMea from PoMea/Magh-H are electroinactive in strong acidic electrolyte (Fig. 8), where an electrochemical response similar to that observed for poly(*o*-methoxyaniline) [21] was expected. This can be due to differences in the structure of the polymer. It has been reported that aniline polymerization into sodium-montmorillonite produces some benzidine type segments and azo bonds in addition of the typical head-to-tail structure of PANI [14,18]. In this case, probably the amount of these segments in PoMea surpasses a critical value, which leads to the generation of an electroinactive material. Also, it is known that as the cross-linking or branching between polymer chains increases, the conductivity and electroactivity decreases. In poly(*o*-methylaniline) there are no polar functional groups that may promote covalent cross-link chains, but it is possible that PoMea created into Magh-H

Table 5
Assignments of FTIR bands of PoMea/Magh-Cu and PoMea/Magh-H nanocomposites

Wavenumbers (cm^{-1})			Assignments
PANI	PoMea/Magh-Cu	PoMea/Magh-H	
3434	3350	3440	N–H stretching
–	2971	2971	C–H stretching of methyl group
	2918	2918	
	2853	2855	
1574	1612	1615	C–C stretching of quinoid ring
1476	1478	1492	C–C stretching of benzenoid ring
1253	1244	1251	C–N stretching
1143	1151	1149	C–H aromatic in-plane bending aromatic
–	1040	1042	Montmorillonite vibrations
	926	929	

PANI band assignments are shown to compare.

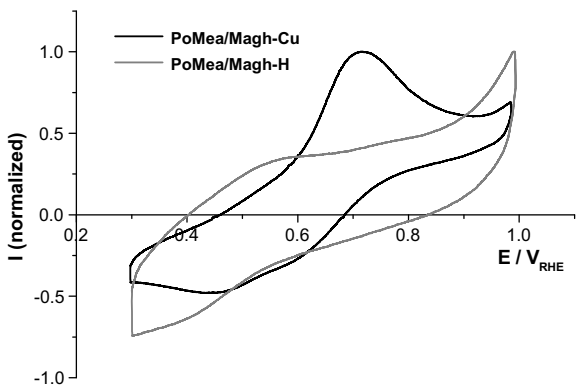

Fig. 8. Cyclic voltammograms of PoMea polymers on glassy carbon electrode in 1 M $HClO_4$ solution. PoMea obtained with Magh-Cu (black line) and PoMea obtained with Magh-H (grey line). Scan rate = 50 mV s^{-1}.

has a higher degree of branching in its structure than that into Magh-Cu. The TG-MS results described above support this hypothesis and the absence of electroactivity of PoMea in comparison to Magh-H can be attributed to a high degree of branching in the polymer structure. TEM results also agree with this argument because the exfoliated morphology of PoMea/Magh-H can also be due to the formation of a voluminous and high molecular weight branched polymer into the clay layers.

4. Conclusions

Nanocomposites with different morphology and consequently different properties have been synthesized. The influence of the cation, intercalated into the clay layers prior to the polymerization, on the properties of the nanocomposites has been analysed. While PoMea/Magh-Cu displayed well-ordered intercalated morphology, PoMea/Magh-H nanocomposites presented an exfoliated one. Furthermore, remarkable differences on the electrochemical properties of the same polymer (PoMea) extracted from the PoMea/Magh-H or PoMea/Magh-Cu nanocomposites have been observed and have been related to differences in the structure of the polymer. Good electrochemical response has been observed for PoMea grown into Magh-Cu in which the cyclic voltammogram shows a broad anodic peak that consists on the overlapping of two redox processes but the one polymerized into Magh-H is electroinactive.

Acknowledgments

The authors thank the financial support from the Ministerio de Educación y Ciencia (MAT2007-60621 Project), Generalitat Valenciana (RED ARVIV2007/076) and the financial support from the Algerian CNEPRU and FNR. H.J.S. thanks MEC for a Juan de la Cierva contract.

References

[1] MacDiarmid AG. Angew Chem Int Ed 2001;40:2581–90.
[2] Joo J, Lee CY. J Appl Phys 2000;88:513–8.
[3] Kuo CT, Kuo HH, Chen SA, Hwang GW. Synth Met 1998;93:155–60.
[4] MacDiarmid AG, Epstein AJ. In: Prasad PN, editor. Frontiers of Polymers and Advanced Materials. New York: Plenum Press; 1984.
[5] Kinlen PJ, Liu J, Graham CR, Remsen EE. Macromolecules 1998;31:1735–44.
[6] Wei ZX, Zhang ZM, Wan MX. Langmuir 2002;18:917–21.
[7] Wei ZX, Wan M. Adv Mater 2002;14:1314–7.
[8] Rao PS, Sathyanarayana DN. Polymer 2002;43:5051–8.
[9] Huang JX, Kaner RB. J Am Chem Soc 2004;126:851–5.
[10] Huang JX, Kaner RB. Angew Chem Int Ed 2004;43:5817–21.
[11] Wu CG, Bein T. Science 1994;264:1757–9.
[12] Yoshimoto S, Ohashi F, Ohnishi Y, Nonami T. Chem Commun 2004;17:1924–5.
[13] Yoshimoto S, Ohashi F, Kameyama T. Macromol Rapid Commun 2004;25:1687–91.
[14] Do Nascimento GM, Constantino VRL, Temperini MLA. Macromolecules 2002;35:7535–7.
[15] Kim BH, Jung JH, Hong SH, Joo J, Epstein AJ, Mizoguchi K, Kim JW, Choi HJ. Macromolecules 2002;35:1419–23.
[16] Kim BH, Hong SH, Joo J, Park IW, Epstein AJ, Kim JW, Choi HJ. J Appl Phys 2004;95:2697–701.

[17] Ballav N, Biswas M. Synth Met 2004;142:309–15.
[18] Do Nascimento GM, Constantino VRL, Landers R, Temperini MLA. Macromolecules 2004;37:9373–85.
[19] Yoshimoto S, Ohashi F, Ohnishi Y, Nonami T. Synth Met 2004;145:265–70.
[20] Yoshimoto S, Ohashi F, Kameyama T. Macromol Rapid Commun 2005;26:461–6.
[21] Boutaleb N, Benyoucef A, Salavagione HJ, Belbachir M, Morallón E. Eur Polym J 2006;42:733–9.
[22] Kim JW, Kim SG, Choi HJ, Jhon MS. Macromol Rapid Commun 1999;20:450–2.
[23] Sung JH, Choi HJ. J Macromol Sci B Phys 2005;44:365–75.
[24] Karaborni S, Smit B, Jeidug W, Urai J, Van Oort E. Science 1996;271:1102–4.
[25] Angelopoulos M, Ray A, MacDiarmid AG, Epstein AJ. Synth Met 1987;21:21–30.
[26] Greenwood NN. In: Chemistry of the elements. Oxford: Butterworth-Heinemann; 1993.
[27] Huang FC, Lee FJ, Lee CK, Chao HP. Colloid Surface A 2004;239:41–7.
[28] Ding Z, Frost R. Thermochim Acta 2004;416:11–6.
[29] Huang MR, Li XG, Yang YL, Wang XS, Yan D. J Appl Polym Sci 2001;81:1838–47.
[30] Li XG, Huang MR, Jin Y, Yang YL. Polymer 2001;42:3427–35.
[31] Housecroft CE, Sharpe AG. Inorganic Chemistry. 2nd ed. Prentice Hall; 2004.
[32] Sariciftci NS, Kuzmany H, Neugebauer H, Neckel A. J Chem Phys 1990;92:4530–9.
[33] Kuszmany H, Sariciftci NS, Neugebauer H, Neckel A. Phys Rev Lett 1988;60:212–5.
[34] Yue J, Wang ZH, Cromack KR, Epstein AJ, MacDiarmid AG. J Am Chem Soc 1991;113:2665–71.
[35] Lindfors T, Ivaska A. J Electroanal Chem 2002;531:43–52.
[36] Viva FA, Andrade EM, Florit MI, Molina FV. Phys Chem Chem Phys 2002;4:2293–300.
[37] Miras MC, Barbero C, Kötz R, Haas O. J Electroanal Chem 1994;369:193–7.
[38] Henderson MJ, Hillman RA, Vieil E. J Phys Chem B 1999;103:8899–907.
[39] Sanchís C, Salavagione HJ, Arias-Pardilla J, Morallón E. Electrochim Acta 2007;52:2978–87.